

# Actinobacillus actinomycetemcomitans Lipopolysaccharide-Mediated Experimental Bone Loss Model for Aggressive Periodontitis

Jill E. Rogers,\* Fei Li,\* Derek D. Coatney,\* Carlos Rossa Jr.,\*† Paul Bronson,† Jaclynn M. Krieder,§ William V. Giannobile,\*|| and Keith L. Kirkwood\*

**Background:** Bacterial constituents, such as Gram-negative derived lipopolysaccharide (LPS), can initiate inflammatory bone loss through induction of host-derived inflammatory cytokines. The aim of this study was to establish a model of aggressive inflammatory alveolar bone loss in rats using LPS derived from the periodontal pathogen *Actinobacillus actinomycetemcomitans*.

**Methods:** Eighteen female Sprague-Dawley rats were divided into LPS test (N = 12) and saline control (N = 6) groups. All animals received injections to the palatal molar gingiva three times per week for 8 weeks. At 8 weeks, linear and volumetric alveolar bone loss was measured by micro-computed tomography ( $\mu$ CT). The prevalence of inflammatory infiltrate, proinflammatory cytokines, and osteoclasts was assessed from hematoxylin and eosin, immunohistochemical, or tartrate-resistant acid phosphatase (TRAP)-stained sections. Statistical analysis was performed.

**Results:** *A. actinomycetemcomitans* LPS induced severe bone loss over 8 weeks, whereas control groups were unchanged. Linear and volumetric analysis of maxillae by  $\mu$ CT indicated significant loss of bone with LPS administration. Histologic examination revealed increased inflammatory infiltrate, significantly increased immunostaining for interleukin IL-6 and -1 $\beta$  and tumor necrosis factor-alpha, and more TRAP-positive osteoclasts in the LPS group compared to controls.

**Conclusion:** Oral injections of LPS derived from the periodontal pathogen *A. actinomycetemcomitans* can induce severe alveolar bone loss and proinflammatory cytokine production in rats by 8 weeks. *J Periodontol* 2007;78:550-558.

## KEY WORDS

*Actinobacillus actinomycetemcomitans*; cytokines; inflammation; lipopolysaccharide; periodontal diseases.

Periodontitis is an oral infectious disease that may result in tooth loss. The hallmark of periodontitis is bone resorption resulting from a host inflammatory response to a bacterial challenge. Periopathogenic bacteria, including *Actinobacillus actinomycetemcomitans*, contain multiple virulence factors, such as lipopolysaccharide (LPS), that can activate the host inflammatory response to initiate alveolar bone resorption.

LPS acts as a microbe-associated molecular pattern recognized through pattern-recognition receptors on resident immune and non-immune cells within the periodontium.<sup>1</sup> This immune response involves recruitment of inflammatory cells, generation of prostanoids and cytokines, elaboration of lytic enzymes, and osteoclast activation.<sup>2,3</sup> Within periodontal tissues and gingival crevicular fluid, activated monocytes, macrophages, and fibroblasts produce classic proinflammatory cytokines, such as interleukin (IL)-1 $\beta$  and -6 and tumor necrosis factor-alpha (TNF- $\alpha$ ).<sup>4-7</sup> These cytokines stimulate matrix metalloproteinases (MMPs; e.g., the collagenases MMP-1, -3, and -13), which destroy tissues through degradation of extracellular matrix components. Moreover, IL-1 and TNF- $\alpha$  induce bone resorption by indirectly stimulating IL-6 or by directly stimulating downstream

\* Department of Periodontics and Oral Medicine, School of Dentistry, University of Michigan, Ann Arbor, MI.

† Department of Diagnosis and Surgery, School of Dentistry at Araraquara, State University of São Paulo, Araraquara, SP, Brazil.

‡ Department of Oral Biology, University at Buffalo, Buffalo, NY.

§ Orthopedics Research Laboratory, University of Michigan.

|| Department of Biomedical Engineering, College of Engineering, University of Michigan.

effectors associated with osteoclastogenesis, such as receptor activator of nuclear factor-kappa B ligand (RANKL). LPS itself can lead to increased osteoblastic expression of prostaglandin E<sub>2</sub>, RANKL, IL-1, and TNF- $\alpha$ .<sup>8</sup> Additionally, in the presence of *A. actinomycetemcomitans*, CD4<sup>+</sup> T cells display an increased expression of RANKL, thereby amplifying osteoclast activation.<sup>9,10</sup>

Activation of the host immune response leads to destruction of the periodontium via cytokine induction. Routinely, IL-1 and -6 and TNF- $\alpha$  are elevated significantly in active versus inactive or healthy sites.<sup>11-15</sup> Also, IL-1 levels have been correlated positively to increased probing depth and clinical attachment loss.<sup>12,14,16</sup>

Small animal models are used commonly in periodontitis studies. In rats, a variety of approaches have been used to create periodontitis, including ligature placement, a soft diet, whole bacteria injection or bacterial oral gavage, and localized LPS injection.<sup>17-22</sup> Although all of these approaches generate inflammation and alveolar bone loss, localized LPS injection may be a more direct and controlled method, because a known amount of inflammatory stimulus is delivered in a titratable manner.<sup>23</sup> However, most studies using the injection model isolated LPS from non-periodontogenic bacteria, such as *Escherichia coli* or *Salmonella typhimurium*.<sup>23-25</sup> The use of *A. actinomycetemcomitans* LPS, as opposed to *E. coli* or *S. typhimurium* LPS, is more relevant to periodontal disease. Recent studies showed that *A. actinomycetemcomitans* can induce inflammatory bone loss in mice.<sup>26,27</sup> *A. actinomycetemcomitans* has been linked to aggressive periodontitis (AP); it was found in AP lesions,<sup>28</sup> AP patients exhibited elevated serum antibodies to *A. actinomycetemcomitans*,<sup>29</sup> and reduction of *A. actinomycetemcomitans* improved the clinical response of AP patients.<sup>30</sup> In particular, serotype b is implicated most often.<sup>31,32</sup> Therefore, to establish an aggressive periodontitis model, we selected *A. actinomycetemcomitans* serotype b (strain Y4). In fact, the serotype determinants of *A. actinomycetemcomitans* Y4 are associated with a high molecular weight LPS-associated antigen.<sup>33</sup> Accordingly, in early-onset periodontitis patients with the highest serum antibody levels to *A. actinomycetemcomitans*, the predominant antibody specificity is to LPS.<sup>34,35</sup> The purpose of this study was to develop a new model for the induction of inflammatory alveolar bone loss in rats, using LPS from the periodontal pathogen *A. actinomycetemcomitans*.

## MATERIALS AND METHODS

### LPS Preparation

LPS was extracted from *A. actinomycetemcomitans* strain Y4 (serotype B) by the hot phenol-water

method as described previously.<sup>36-38</sup> The bacteria were treated sequentially with lysozyme, DNase, RNase, and proteases to extract and isolate the LPS. The LPS used in the present study contained <0.001% nucleic acid by spectrophotometry and ~0.7% protein by bicinchoninic acid protein assay. The paucity of protein in the LPS preparations was verified by polyacrylamide gel electrophoresis and subsequent staining with silver nitrate and Coomassie blue (Fig. 1). Gas chromatography/mass spectrometry of the fatty acids present in the *A. actinomycetemcomitans* LPS preparations was performed. All peaks present in the preparation after transmethylated were identified by analysis of the mass spectral patterns as described previously.<sup>39</sup>

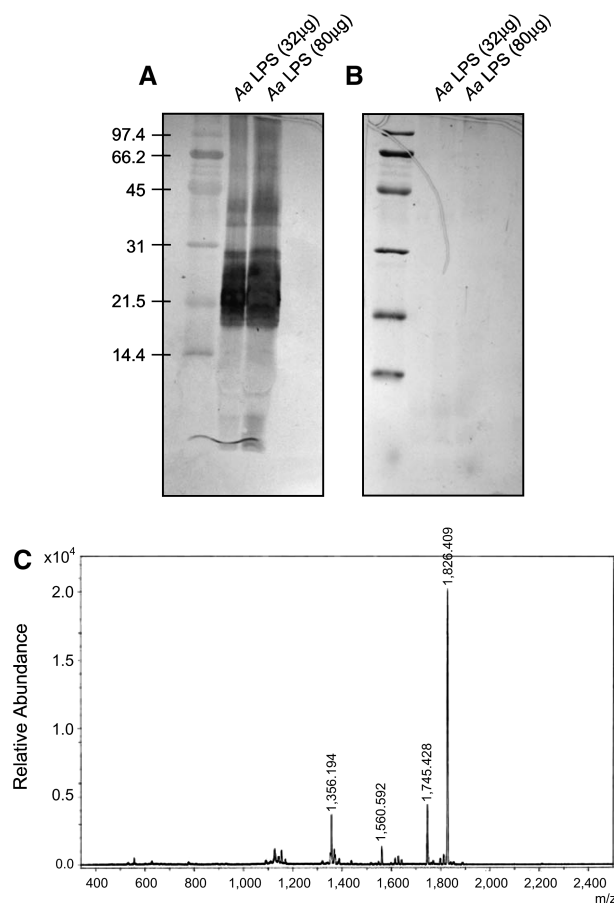


**Figure 1.**

Characterization of *A. actinomycetemcomitans* LPS used in these studies. **A)** Purified *A. actinomycetemcomitans* LPS demonstrated characteristic laddering on a silver nitrate-stained polyacrylamide gel with indicated quantities of *A. actinomycetemcomitans* LPS. **B)** Absence of protein as indicated by Coomassie-stained gel with the same LPS. **C)** Matrix-assisted laser desorption/ionization-time of flight (MALDI-TOF) mass spectra showing singly charged anions representing the major lipid A structures present. The major peak corresponds to the hexa-acylated form (mass-to-charge ratio [m/z] at 1,827) with minor forms being present as well.

## Animals

Based on data from previous studies using experimental periodontal disease models,<sup>40,41</sup> the estimated minimal sample size for detecting a difference of 50% between two groups is six animals per group. This was calculated considering a power of 80%, *P* value of 0.05, normal distribution, and equivalent variances of the experimental and control groups.

Female adult Sprague-Dawley rats<sup>¶</sup> (~250 g each) were housed in pairs under specific pathogen-free conditions with food and tap water *ad libitum*. Once weekly, animals were weighed to ensure proper growth and nutrition.

Injections were given three times each week for 8 weeks. First, anesthesia was induced with 4% to 5% isoflurane and maintained with 1% to 2% isoflurane. All rats received 2  $\mu$ l total volume of solution via a 33-gauge Hamilton syringe to the palatal interproximal gingiva between the first, second, and third molars. The test group (N = 12) received 10  $\mu$ g/ $\mu$ l *A. actinomycetemcomitans* LPS, whereas the control group (N = 6) received neutral 1 $\times$  phosphate buffered saline.

At 8 weeks, all animals were sacrificed by carbon dioxide asphyxiation. The maxillae were hemisected, and posterior block sections were immersed directly in 10% buffered formalin fixative solution for 72 hours. All protocols were approved by the University Committee on the Use and Care of Animals at the University of Michigan.

## Micro-Computed Tomography

Non-demineralized rat maxillae were scanned in 70% ethanol by a cone beam micro-computed tomography ( $\mu$ CT) system.<sup>#</sup> Each scan was reconstructed at a mesh size of 18  $\mu$ m<sup>3</sup>, and three-dimensional digitized images were generated for each specimen. By using software,<sup>\*\*</sup> it is possible to view the scans from virtually any angle or cross-section. Therefore, a standardized orientation of the images was necessary prior to measurement. First, the buccal and palatal plates were made horizontal with the x-axis. Then the x-plane was oriented so that it crossed through the palatal roots. Parallelism of the molar cusps with the x-axis was used for verification of alignment. A threshold of 1,621 was set to distinguish between mineralized and non-mineralized tissue in all scans.

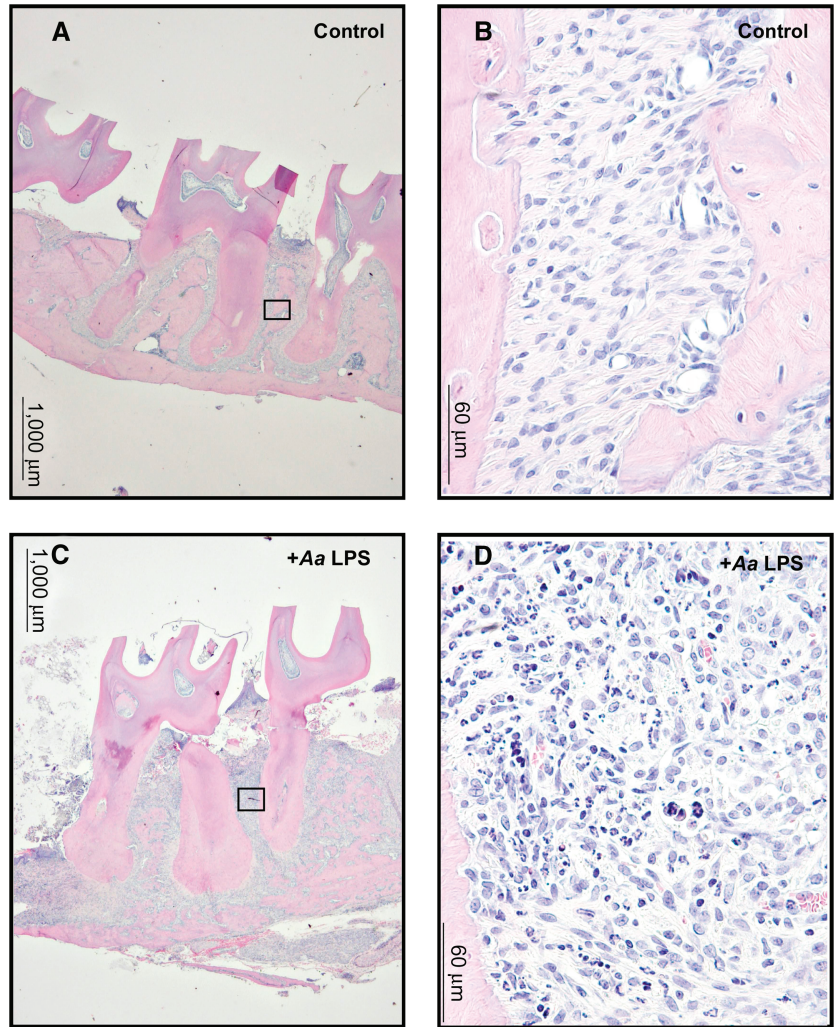


**Figure 2.**

*A. actinomycetemcomitans* LPS induced more inflammatory cell infiltrate into the area adjacent to bone loss. Histologic appearance of representative control at low magnification (A), and at high magnification (B), enlarged box area from A shows normal structure with minimal inflammatory cells. *A. actinomycetemcomitans* LPS-injected rat periodontal tissues at low magnification (C), and at high magnification (D), enlarged box area from C shows significant inflammatory infiltrate is present.

Linear measurements were taken between the first and second molars, from cemento-enamel junction (CEJ) to alveolar bone crest (ABC), as described by Park et al.<sup>22</sup> Loss of bone volume was assessed using three-dimensional isoform displays. After proper image orientation, the region of interest (ROI) was designated. Width of the ROI was measured at the height of contour of the molars. Height of the ROI was measured from molar cusp tips to root apices. The depth was equal to the bucco-lingual size of the teeth plus 100 voxels (1.8 mm<sup>3</sup>). After establishing the

<sup>¶</sup> Charles River, Wilmington, MA.

<sup>#</sup> GE Healthcare BioSciences, Chalfont St. Giles, U.K.

<sup>\*\*</sup> GEHC MicroView software, version Viz+ 2.0 build 0029, GE Healthcare, Chalfont St. Giles, U.K.

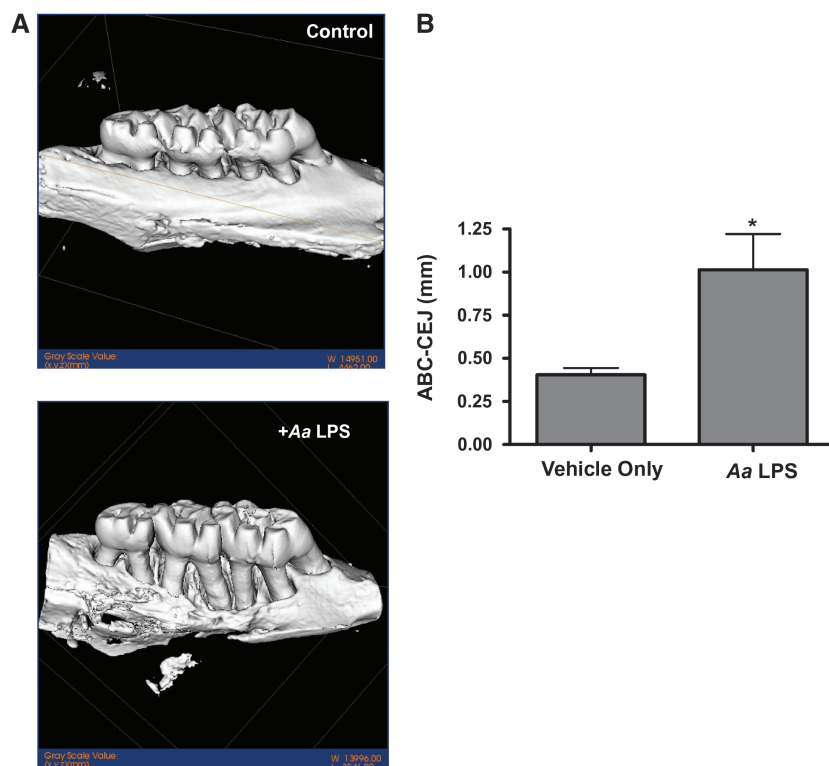


**Figure 3.**

$\mu$ CT shows *A. actinomycetemcomitans* LPS induced significant linear bone loss. **A)** Reformatted  $\mu$ CT isoform display from 8-week *A. actinomycetemcomitans* LPS-injected rat maxillae exhibits dramatic palatal and interproximal bone loss. **B)** Linear bone loss as measured from the CEJ to the ABC. Significant bone loss (\* $P < 0.01$ ) was observed between control ( $N = 6$ ) and *A. actinomycetemcomitans* LPS (Aa LPS)-injected rats ( $N = 12$ ).

threshold at 1,621, the bone volume fraction was calculated and expressed as the amount of remaining bone in ROI/ROI.

#### Immunohistochemistry and Tartrate-Resistant Acid Phosphatase Staining

Formalin-fixed specimens were decalcified in 10% EDTA solution at 4°C for 2 weeks. The EDTA solution was changed three times per week. The maxillae were embedded in paraffin and 5- $\mu$ m sections were prepared.

A few sections from each group were stained with hematoxylin and eosin (H&E) for visualization of the inflammatory infiltrate. Images were captured using an inverted microscope<sup>††</sup> and camera.<sup>‡‡</sup>

Immunohistochemical staining for IL-6 and -1 $\beta$  and TNF- $\alpha$  was performed on tissue sections for both groups. Deparaffinized tissue sections were placed in antigen retrieval buffer<sup>§§</sup> (in a pressure chamber<sup>|||</sup> for 15 minutes, then removed and cooled to room temperature. Primary antibodies of anti-rat IL-6, anti-rat IL-1 $\beta$ , and anti-rat TNF- $\alpha$  monoclonal antibodies<sup>¶¶</sup> were used (1:200 each antibody). Cytokine presence

was detected using reagent<sup>##</sup> and red stain<sup>\*\*\*</sup> per manufacturer's instructions. Coverslips were seated on each slide with histologic mounting medium.<sup>†††</sup> Control sections were incubated with preimmunoserum to assess background staining. Images of the specimens were captured using the inverted scope and camera.

The digitized slide images were displayed on a computer screen for scoring by two independent examiners. Examiners were calibrated by comparing images of a known intensity to a standardized score sheet containing representative slides of one-, two-, three-, or four-color intensity. All slides were displayed in random order and assigned a score of 1, 2, 3, or 4; "1" represented 0% to 20% positive red stain, "2" represented 20% to 40% positive stain, "3" represented 40% to 60% positive stain, and "4" represented >60% positive stain.

For detection of osteoclasts, tartrate-resistant acid phosphatase (TRAP) staining was performed for both groups using a leukocyte acid phosphatase kit.<sup>‡‡‡</sup> Active osteoclasts were defined as multinucleated TRAP-positive cells in contact with the bone surface. Slides from similar sagittal sections were used to enumerate TRAP-positive cells.

#### Statistical Analysis

Differences among data were found by one-way analysis of variance (ANOVA) or post hoc analysis with the Bonferroni test where indicated.  $P$  values <0.05 were considered significant.

## RESULTS

#### Analysis of *A. actinomycetemcomitans* LPS

The *A. actinomycetemcomitans* LPS used in this study contained no nucleic acid and minimal protein. The absence of protein in *A. actinomycetemcomitans* LPS preparations was confirmed by polyacrylamide gel electrophoresis of extract samples and Coomassie staining (Figs. 1A and 1B). The carbohydrate moieties and lipid A fraction were visualized by silver

†† Nikon TS100, Nikon, Melville, NY.

‡‡ Nikon CCD 5.1 megapixels, Nikon.

§§ Dako, Glostrup, Denmark.

||| Biocare Medical, Concord, CA.

¶¶ R&D Systems, Minneapolis, MN.

## Vectastain Elite ABC, Vector Labs, Burlingame, CA.

\*\*\* Nova Red, Vector Labs.

††† Permount, Fisher Scientific, Pittsburg, PA.

‡‡‡ Sigma, St. Louis, MO.

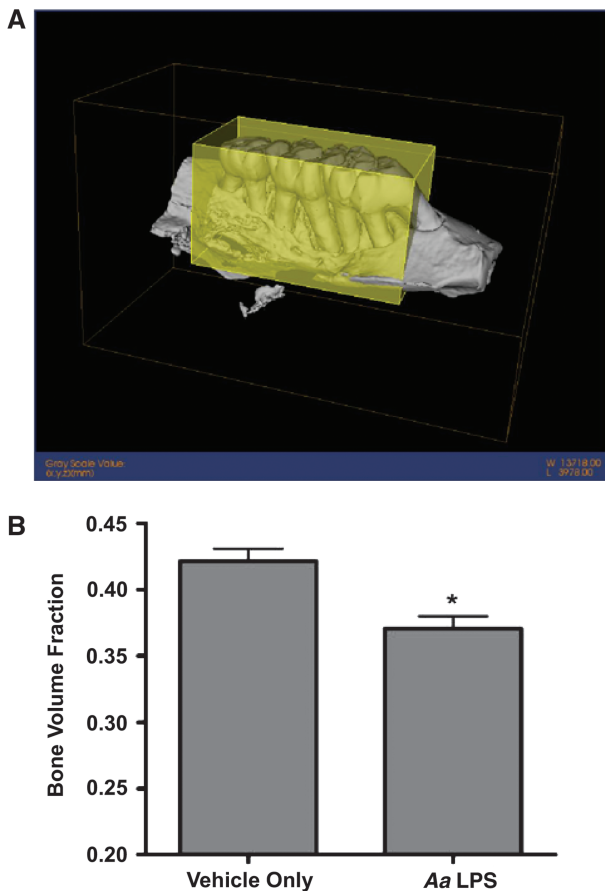


#### Figure 4.

*A. actinomycetemcomitans* LPS induced significant loss of proximal bone volume. **A)** Reformatted  $\mu$ CT isoform display showing volumetric ROI used for analysis. **B)** Analysis of  $\mu$ CT volumes were assessed using software. Data are presented as percentage bone within ROI. Significant bone loss (\* $P < 0.001$ ) was observed between control ( $N = 6$ ) and *A. actinomycetemcomitans* LPS (*Aa* LPS)-injected rats ( $N = 12$ ).

nitrate-stained gels. Lipid A content also was analyzed by gas chromatography/mass spectrometry. As shown in Figure 1C, the fatty acids found in the preparation were identified by the mass spectral patterns. The predominant major mass ion should be 1,827, which corresponds to a hexa-acylated diphosphorylated lipid A. Most of the LPS preparation contains this species as observed previously.<sup>41</sup> The peak at 1,745 corresponds to a monophosphorylated species (natural or created by the extraction procedures), whereas peaks at 1,560 and 1,356 correspond to the penta- and tetra-acylated species. The amounts of this minor species are small compared to the predominant  $m/z$  at 1,827.

#### *A. actinomycetemcomitans* LPS Induced Inflammatory Infiltrate

The maxillae were fixed and embedded for histologic staining by H&E. Sections from *A. actinomycetemco-*

*mitans* LPS-injected rats displayed significantly greater inflammatory cell infiltrate (localized to the connective tissue proximal to the junctional epithelium and the surrounding alveolar crest) compared to sections from vehicle-injected rats (Fig. 2). These data illustrate that more inflammatory cells, predominantly neutrophils and macrophages, were present in the LPS-injected tissues, whereas relatively fewer inflammatory cells were present in the vehicle-injected controls.

#### *A. actinomycetemcomitans* LPS Induced Significant Alveolar Bone Loss

To evaluate the extent of alveolar bone loss and periodontal destruction,  $\mu$ CT was used as described by Park et al.<sup>22</sup> Three-dimensional reformatted  $\mu$ CT images from 8-week specimens revealed a dramatic difference in the amount of bone destruction of the maxillae (Fig. 3A, lower panel). In the rats that received vehicle only, there was minimal bone loss compared to non-injected rats (Fig. 3A, upper panel). In the vehicle-injected controls, the alveolar crest was in the coronal one-third of the roots, paralleling the CEJs of the teeth. In contrast, specimens from the *A. actinomycetemcomitans* LPS-injected group displayed a virtual obliteration of the palatal and interproximal bone. The bony crest was located near the molar apices, in a U-shaped configuration. The greatest vertical destruction corresponded to the site of LPS injection (the interproximal area between the molar teeth).

Linear measurements from CEJs to ABCs revealed mean bone losses of 0.405 mm in control animals and 1.04 mm in LPS-injected animals (Fig. 3). The overall difference (0.634 mm) was statistically significant ( $P < 0.01$ ) as assessed by one-way ANOVA.

For volumetric analysis, an ROI (highlighted area in Fig. 4A) was used to determine the bone volume fraction. By this unbiased approach, the bone volume fraction was 0.42 for the vehicle group and 0.37 for the LPS group (Fig. 4B). This difference was significant ( $P < 0.01$ ) by one-way ANOVA.

#### *A. actinomycetemcomitans* LPS Induced Inflammatory Cytokine Expression

To establish this periodontal model as an inflammatory bone loss model, it was critical to characterize inflammatory cytokine expression. Immunostaining for selected key proinflammatory cytokines showed marked differences between *A. actinomycetemcomitans* LPS-treated and control samples (Fig. 5). Relative values were assigned using a graded scoring system. The scores of "1" are from vehicle-injected control animals (upper panels of Figs. 5A, 5C, and 5E), whereas a "4" score was given to the *A. actinomycetemcomitans* LPS-injected group (lower panels of Figs. 5A, 5C, and 5E). A score of "0" was included

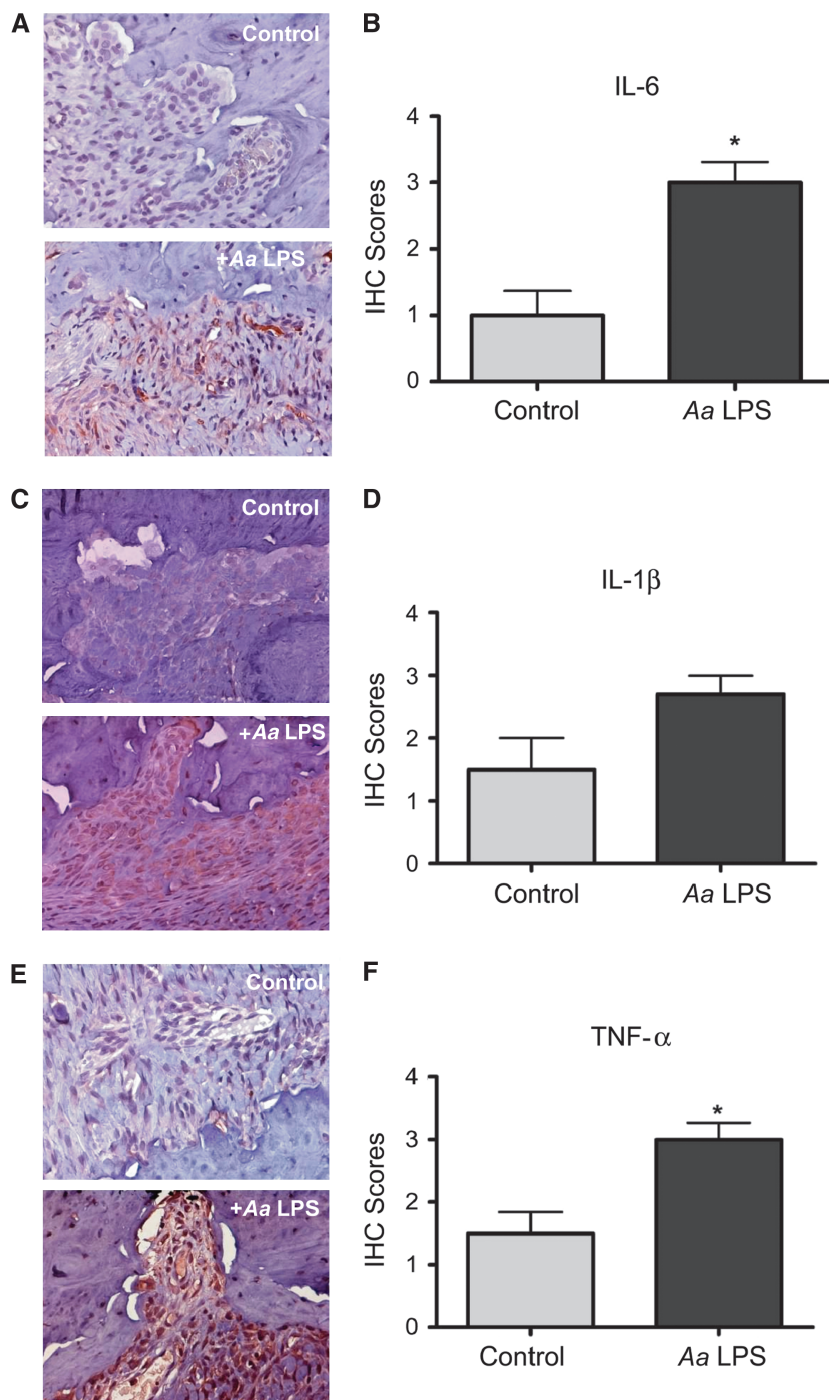


### Figure 5.

Pronounced expression of proinflammatory cytokines was observed in *A. actinomycetemcomitans* LPS (Aa LPS)-injected animals. Histologic sections were immunostained and detected using Nova Red reagent for IL-6 (A), IL-1β (C), or TNF-α (E). B, D, and F Immunohistochemical (IHC) scores from control animals and 8 weeks post-LPS injections. Significant differences were observed for IL-6 (\* $P = 0.0104$ ) and TNF-α (\* $P = 0.0305$ ) and approached significant differences between control and LPS-treated groups for IL-1β ( $P = 0.0671$ ). (Original magnification  $\times 60$ .)

as background staining from preimmune serum (data not shown). For IL-6, the control group had a mean score of 1.0 (range, 0 to 2), whereas the LPS group had a mean score of 3.0 (range 2 to 4) (Fig. 5B). The difference was similar for IL-1β (1.5 [range, 0 to 3] and 2.75 [range, 1 to 4], respectively) (Fig. 5D) and TNF-α (1.5 [range, 0 to 2] and 3 [range, 2 to 4], respectively) (Fig. 5F). Scores of “4,” reflecting the greatest prevalence of cytokine, were distributed only among the *A. actinomycetemcomitans* LPS-injected group.

### *A. actinomycetemcomitans* LPS Increased Osteoclastogenesis and Bone Resorption

Histologic examination and TRAP staining were performed to quantify osteoclastogenesis. Without *A. actinomycetemcomitans* LPS injection, few osteoclasts were detected (Fig. 6). However, significantly more osteoclasts were noted ( $P = 0.0023$ ) after 8 weeks of *A. actinomycetemcomitans* LPS exposure.

### DISCUSSION

In the present study, we established a new model of aggressive periodontal disease in rats through localized injection of highly purified *A. actinomycetemcomitans* LPS. At 8 weeks, evidence of periodontal disease included increased inflammatory cell infiltrate, enhanced inflammatory cytokine expression, and stimulation of osteoclastogenesis manifesting as significant alveolar bone loss.

We used  $\mu$ CT for the analysis of bone area and volume. One of the distinct advantages of this novel technique is the use of the same specimens for histologic examination following  $\mu$ CT scanning. Moreover, the quality of the digital data facilitates an easier assessment than when using defleshed specimens. Park et al.<sup>22</sup> showed that three-dimensional  $\mu$ CT imaging for linear and volumetric parameter assessment (height, volume, mineral content, mineral density, and bone volume fraction) was highly reliable and reproducible with an intraclass correlation coefficient of  $>0.99$ . This suggested that three-dimensional alveolar bone measurements might provide greater accuracy than conventional

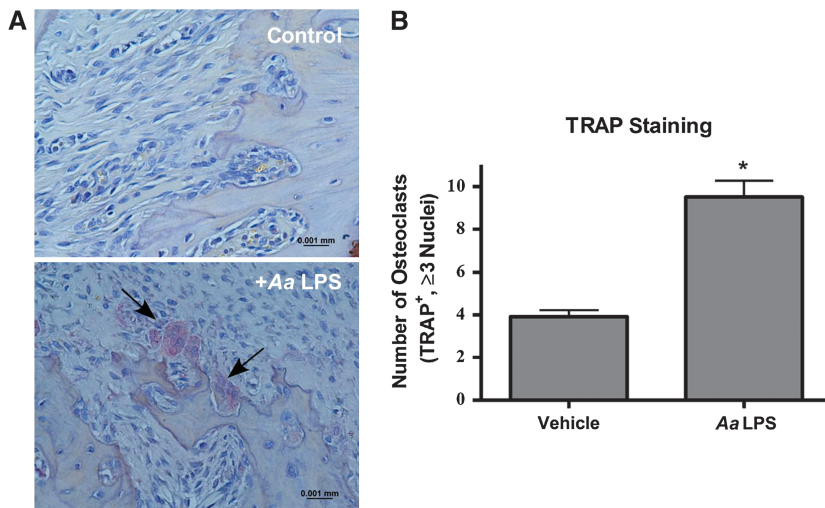


### Figure 6.

*A. actinomycetemcomitans* LPS delivery enhanced osteoclastogenesis. **A)** Histologic sections were stained for TRAP. Arrows indicate TRAP-positive cells in *A. actinomycetemcomitans* LPS (Aa LPS)-injected rats. **B)** Stained cells that were TRAP-positive and had three or more nuclei were enumerated. LPS-injected animals ( $N = 12$ ) exhibited significantly more TRAP-positive cells than control animals ( $N = 6$ ;  $*P = 0.0023$ ). (Scale bar = 1  $\mu\text{m}$ ; original magnification  $\times 60$ .)

two-dimensional methods. Future studies could use in vivo  $\mu\text{CT}$  to document better progressive bone loss or gain.

Consistent with the observation of severe bone loss, there was a significant increase in the number of osteoclasts. Because rat molars undergo distal drift, there is constant resorptive activity on the proximal bone; therefore, osteoclasts were enumerated only on the distal aspect of the interproximal bone.<sup>42,43</sup> Analysis following LPS injection showed that the number of osteoclasts was relatively small ( $<10$ ); however, this number was not corrected per millimeter of bone surface. The low number also may reflect the nature of the experimental design; after an 8-week period of LPS-induced bone loss, most of the osteoclastic bone resorption already has occurred and the osteoclasts have undergone apoptosis. Nevertheless, the increase in osteoclast count correlated well with the linear and volumetric measurements of alveolar bone loss.

The impetus for the development of a new small animal periodontitis model is the relative lack of such models exhibiting robust amounts of inflammatory bone loss with relevant periodontal pathogens. A major limitation of the majority of *Porphyromonas gingivalis* infection models (versus LPS injection) is the minimal amount of bone loss that occurs; mice and rats display only fractions of a millimeter of bone loss over the observation periods.<sup>44,45</sup> Such minute bone loss, typically  $<10\%$  to  $20\%$  of the root length, hinders evaluation of therapeutic treatment effects. Also, models described using *E. coli* endotoxin<sup>23</sup> or ligature-

induced disease<sup>39,40</sup> resulted in very rapid and severe bone destruction (typically  $>50\%$  bone loss) over a 1- to 2-week period. These models represented acute models of bone resorption, thereby truncating the timeframe available for observing therapeutic efficacy. The amount of linear bone loss ( $\sim 1$  mm) created by *A. actinomycetemcomitans* LPS over an 8-week period was more than that created by *E. coli* LPS injected daily over an 8-day period<sup>23</sup> and slightly more than *E. coli* LPS micropipetted daily into rat gingival sulci over an 8-week observation period (0.65 mm difference).<sup>39</sup>

*A. actinomycetemcomitans* whole bacteria injection models recently were used in C57/BL6 mice.<sup>26</sup> Proinflammatory cytokine expression, primarily T helper 1-type TNF- $\alpha$ , was elevated significantly in the first 30 days postinfection but it decreased in the last 30 days. In the present study, we observed consistently high inflammatory cytokine expression throughout a 60-day

period. This is similar to other oral pathogen-induced bone loss models<sup>26,46</sup> and consistent with the ability of *A. actinomycetemcomitans* LPS to induce TNF- $\alpha$  and IL-1 $\beta$  and -6 in vitro.<sup>47</sup> Other in vitro data from our research group showed that *A. actinomycetemcomitans* LPS can stimulate RANKL, IL-6, and MMP-13 expression as well as several periodontally relevant cells, including periodontal ligament fibroblasts, osteoblasts, and macrophages.<sup>44,45,48</sup>

Female Sprague-Dawley rats were selected because of the preferred pharmacodynamics of a therapeutic used in a parallel-arm experiment. The amount of inflammation present may have been affected by female sex hormones, yet the exact nature and mechanism of such effects are largely unknown. In oophorectomized Sprague-Dawley rats, daily injections of estrogen and/or progesterone produced no difference in infiltration of mononuclear cells or epithelial downgrowth compared to vehicle-injected sham-operated controls.<sup>49</sup> Recently, administration of 17 $\beta$ -estradiol prevented ethanol-induced bone loss in female Sprague-Dawley rats by blocking osteoblastic RANKL mRNA induction and osteoclastogenesis.<sup>50</sup> In our study, all animals were of the same age and gender and were assigned randomly, nullifying intergroup differences. With sufficient sample size, intragroup differences are negated as well.

## CONCLUSIONS

We demonstrated that LPS endotoxin from the periodontal pathogen *A. actinomycetemcomitans* initiated

severe alveolar bone loss. Significant elevations in inflammatory cytokines and osteoclastogenesis were consistent with the observed advanced bony destruction. The use of a well-established animal model of periodontal disease, as demonstrated in this study, will permit future evaluation of experimental therapeutics that target inflammatory alveolar bone loss.

## ACKNOWLEDGMENTS

The authors thank Richard Darveau, professor, Oral Biology and Periodontics, University of Washington, for LPS analysis; Nisha D'Silva, assistant professor, Periodontics and Oral Medicine, University of Michigan, for discussions of descriptive histology; and Zach Abramson, University of Michigan, for input on  $\mu$ CT analysis. This work was supported by Scios, Mountain View, CA, Department of Defense W81XWH-05-0075 to KLK, National Institutes of Health DE 016619 and DE 13397 to WVG, and National Institutes of Health P30-AR46024.

## REFERENCES

- Akira S, Hemmi H. Recognition of pathogen-associated molecular patterns by TLR family. *Immunol Lett* 2003; 85:85-95.
- Genco CA, Van Dyke T, Amar S. Animal models for *Porphyromonas gingivalis*-mediated periodontal disease. *Trends Microbiol* 1998;6:444-449.
- Listgarten MA, Wong MY, Lai CH. Detection of *Actinobacillus actinomycetemcomitans*, *Porphyromonas gingivalis*, and *Bacteroides forsythus* in an *A. actinomycetemcomitans*-positive patient population. *J Periodontol* 1995;66:158-164.
- Lee HJ, Kang IK, Chung CP, Choi SM. The subgingival microflora and gingival crevicular fluid cytokines in refractory periodontitis. *J Clin Periodontol* 1995;22: 885-890.
- Leng SX, Elias JA. Interleukin-11 inhibits macrophage interleukin-12 production. *J Immunol* 1997;159:2161-2168.
- Chen C, Chang K, Huang J, Huang J, Tsai C. Interleukin-6 production by human gingival fibroblasts following stimulation with *Actinobacillus actinomycetemcomitans*. *Kaohsiung J Med Sci* 1998;14:367-378.
- Tsai C, Ho Y, Chen C. Levels of interleukin-1 beta and interleukin-8 in gingival crevicular fluids in adult periodontitis. *J Periodontol* 1995;66:852-859.
- Roux S, Orcel P. Bone loss. Factors that regulate osteoclast differentiation: An update. *Arthritis Res* 2000; 2:451-456.
- Mahamed DA, Marleau A, Alnaeeli M, et al. G(-) anaerobes-reactive CD4+ T-cells trigger RANKL-mediated enhanced alveolar bone loss in diabetic NOD mice. *Diabetes* 2005;54:1477-1486.
- Teng YT, Nguyen H, Gao X, et al. Functional human T-cell immunity and osteoprotegerin ligand control alveolar bone destruction in periodontal infection. *J Clin Invest* 2000;106:R59-R67.
- Ejeil AL, Gaultier F, Igondjo-Tchen S, et al. Are cytokines linked to collagen breakdown during periodontal disease progression? *J Periodontol* 2003;74: 196-201.
- Gamonal J, Acevedo A, Bascones A, Jorge O, Silva A. Levels of interleukin-1 beta, -8, and -10 and RANTES in gingival crevicular fluid and cell populations in adult periodontitis patients and the effect of periodontal treatment. *J Periodontol* 2000;71:1535-1545.
- Geivelis M, Turner DW, Pederson ED, Lamberts BL. Measurements of interleukin-6 in gingival crevicular fluid from adults with destructive periodontal disease. *J Periodontol* 1993;64:980-983.
- Gorska R, Gregorek H, Kowalski J, Laskus-Perendyk A, Syczewska M, Madalinski K. Relationship between clinical parameters and cytokine profiles in inflamed gingival tissue and serum samples from patients with chronic periodontitis. *J Clin Periodontol* 2003;30:1046-1052.
- Stashenko P, Jandinski JJ, Fujiyoshi P, Rynar J, Socransky SS. Tissue levels of bone resorptive cytokines in periodontal disease. *J Periodontol* 1991;62: 504-509.
- Engelbrecht SP, Hey-Hadavi J, Ehrhardt FJ, et al. Gingival crevicular fluid levels of interleukin-1beta and glycemic control in patients with chronic periodontitis and type 2 diabetes. *J Periodontol* 2004;75:1203-1208.
- Klausen B. Microbiological and immunological aspects of experimental periodontal disease in rats: A review article. *J Periodontol* 1991;62:59-73.
- Robinson M, Hart D, Pigott G. The effects of diet on the incidence of periodontitis in rats. *Lab Anim* 1991;25: 247-253.
- Fiehn N, Klausen B, Evans R. Periodontal bone loss in *Porphyromonas gingivalis*-infected specific pathogen-free rats after preinoculation with endogenous *Streptococcus sanguis*. *J Periodontol Res* 1992; 27:609-614.
- Llavaneras A, Golub LM, Rifkin BR, et al. CMT-8/clodronate combination therapy synergistically inhibits alveolar bone loss in LPS-induced periodontitis. *Ann N Y Acad Sci* 1999;878:671-674.
- Baker PJ. The role of immune responses in bone loss during periodontal disease. *Microbes Infect* 2000;2: 1181-1192.
- Park C, Abramson Z, Taba M, et al. Three-dimensional micro-computed tomographic imaging of alveolar bone in experimental bone loss or repair. *J Periodontol* 2007;78:273-281.
- Ramamurthy NS, Xu JW, Bird J, et al. Inhibition of alveolar bone loss by matrix metalloproteinase inhibitors in experimental periodontal disease. *J Periodontol Res* 2002;37:1-7.
- Llavaneras A, Ramamurthy NS, Heikkila P, et al. A combination of a chemically modified doxycycline and a bisphosphonate synergistically inhibits endotoxin-induced periodontal breakdown in rats. *J Periodontol* 2001;72:1069-1077.
- Dumitrescu AL, Abd-El-Aleem S, Morales-Aza B, Donaldson LF. A model of periodontitis in the rat: Effect of lipopolysaccharide on bone resorption, osteoclast activity, and local peptidergic innervation. *J Clin Periodontol* 2004;31:596-603.
- Garlet GP, Avila-Campos MJ, Milanezi CM, Ferreira BR, Silva JS. *Actinobacillus actinomycetemcomitans*-induced periodontal disease in mice: Patterns of cytokine, chemokine, and chemokine receptor expression and leukocyte migration. *Microbes Infect* 2005;7: 738-747.



27. Garlet GP, Cardoso CR, Silva TA, et al. Cytokine pattern determines the progression of experimental periodontal disease induced by *Actinobacillus actinomycescomitans* through the modulation of MMPs, RANKL, and their physiological inhibitors. *Oral Microbiol Immunol* 2006;21:12-20.
28. Albandar J, Olsen I, Gjermeo PI, et al. Associations between six DNA probe-detected periodontal bacteria and alveolar bone loss and other clinical signs of periodontitis. *Acta Odontol Scand* 1990;48:415-423.
29. Genco R, Zambon J, Murray PA. Serum and gingival fluid antibodies as adjuncts in the diagnosis of *Actinobacillus actinomycescomitans*-associated periodontal disease. *J Periodontol* 1985;56:41-50.
30. Christersson L, Slots J, et al. Microbiological and clinical effects of surgical treatment of localized juvenile periodontitis. *J Clin Periodontol* 1985;12:465-476.
31. Zambon J, Slots J, et al. Serology of oral *Actinobacillus actinomycescomitans* and serotype distribution in human periodontal disease. *Infect Immun* 1983;41:19-27.
32. Yang H, Asikainen S, et al. Relationship of *Actinobacillus actinomycescomitans* serotype b to aggressive periodontitis: Frequency in pure cultured isolates. *J Periodontol* 2004;75:592-599.
33. Califano J, Schenkein H, et al. Immunodominant antigen of *Actinobacillus actinomycescomitans* Y4 in high-responder patients. *Infect Immun* 1989;57:1582-1589.
34. Califano J, Schenkein H, et al. Immunodominant antigens of *Actinobacillus actinomycescomitans* serotype b in early-onset periodontitis patients. *Oral Microbiol Immunol* 1992;7:65-70.
35. Wilson ME, Hamilton RG. Immunoglobulin G subclass response of localized juvenile periodontitis patients to *Actinobacillus actinomycescomitans* Y4 lipopolysaccharide. *Infect Immun* 1992;60:1806-1812.
36. Darveau R, Hancock R. Procedure for isolation of bacterial lipopolysaccharides from both smooth and rough *Pseudomonas aeruginosa* and *Salmonella typhimurium* strains. *J Bacteriol* 1983;155:831-838.
37. Westphal O, Jann K. Bacterial lipopolysaccharide extraction with phenol water and further application of these procedures. *Methods Carbohydr Chem* 1965;5:83-91.
38. Darveau RP, Pham TT, Lemley K, et al. *Porphyromonas gingivalis* lipopolysaccharide contains multiple lipid A species that functionally interact with both toll-like receptors 2 and 4. *Infect Immun* 2004;72:5041-5051.
39. Chang K, Ramamurthy NS, McNamara T. Tetracyclines inhibit *Porphyromonas gingivalis*-induced alveolar bone loss in rats by a non-antimicrobial mechanism. *J Periodontol* 1994;29:242-249.
40. Karimbux NY, Ramamurthy NS, Golub LM, Nishimura I. The expression of collagen I and XII mRNAs in *Porphyromonas gingivalis*-induced periodontitis in rats: The effect of doxycycline and chemically modified tetracycline. *J Periodontol* 1998;69:34-40.
41. Guo L, Lim KB, Gunn JS, et al. Regulation of lipid A modifications by *Salmonella typhimurium* virulence genes phoP-phoQ. *Science* 1997;276:250-253.
42. Roux D, Meunier C, Woda A. A biometric analysis in the rat of the horizontal component of physiological tooth migration and its response to altered occlusal function. *Arch Oral Biol* 1993;38:957-963.
43. Graves DT, Liu R, Alikhani M, Al-Mashat H, Trackman PC. Diabetes-enhanced inflammation and apoptosis – Impact on periodontal pathology. *J Dent Res* 2006;85:15-21.
44. Rossa C Jr., Liu M, Patil C, Kirkwood KL. MKK3/6-p38 MAPK negatively regulates murine MMP-13 gene expression induced by IL-1beta and TNF-alpha in immortalized periodontal ligament fibroblasts. *Matrix Biol* 2005;24:478-488.
45. Patil C, Rossa C Jr., Kirkwood KL. *A. actinomycescomitans* LPS induces IL-6 expression through multiple MAPK pathways in periodontal ligament fibroblasts. *Oral Microbiol Immunol* 2006;21:392-398.
46. Hong CY, Lin SK, Kok SH, et al. The role of lipopolysaccharide in infectious bone resorption of periapical lesion. *J Oral Pathol Med* 2004;33:162-169.
47. Schytte Blix IJ, Helgeland K, Hvattum E, Lyberg T. Lipopolysaccharide from *Actinobacillus actinomycescomitans* stimulates production of interleukin-1beta, tumor necrosis factor-alpha, interleukin-6 and interleukin-1 receptor antagonist in human whole blood. *J Periodontol Res* 1999;34:34-40.
48. Rossa C Jr., Ehman K, Liu M, Patil C, Kirkwood K. MKK3/6-p38 MAPK signaling is required for IL-1beta and TNF-alpha-induced RANKL expression in bone marrow stromal cells. *J Interferon Cytokine Res* 2006;26:719-729.
49. Lundgren D, Magnusson B, Lindhe J. Connective tissue alterations in gingivae of rats treated with estrogen and progesterone. *Odontol Revy* 1973;24:49-58.
50. Chen J, Haley RL, et al. Estradiol protects against ethanol-induced bone loss by inhibiting upregulation of RANKL in osteoblasts. *J Pharmacol Exp Ther* 2006;319:1182-1190.

Correspondence: Dr. Keith L. Kirkwood, Department of Periodontics and Oral Medicine, University of Michigan, 3349 Dental, 1011 N. University Ave., Ann Arbor, MI 48109-1078. Fax: 734/763-5503; e-mail: kkkirk@umich.edu.

Accepted for publication September 29, 2006.